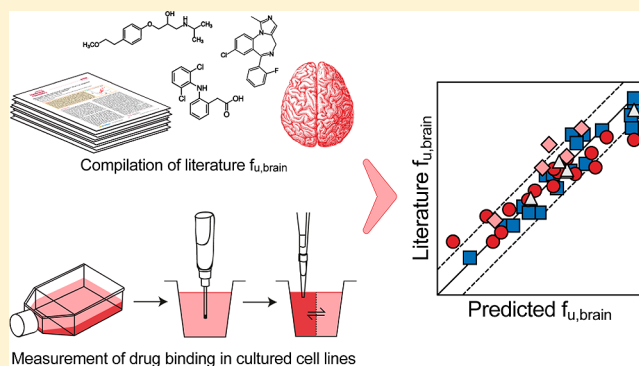


A High-Throughput Cell-Based Method to Predict the Unbound Drug Fraction in the Brain

André Mateus,^{†,‡} Pär Matsson,^{†,§,||} and Per Artursson^{*,†,§,||}[†]Department of Pharmacy, Uppsala University, SE-751 23 Uppsala, Sweden[‡]Research Institute for Medicines and Pharmaceutical Sciences (iMed.Ulisboa), Faculty of Pharmacy, University of Lisbon, 1649-003 Lisbon, Portugal[§]Uppsala University Drug Optimization and Pharmaceutical Profiling Platform (UDOPP)—a node of the Chemical Biology Consortium Sweden, Uppsala University, 751 23 Uppsala, Sweden^{||}Science for Life Laboratory Drug Discovery and Development Platform, Uppsala University, 751 23 Uppsala, Sweden

S Supporting Information

ABSTRACT: Optimization of drug efficacy in the brain requires understanding of the local exposure to unbound drug at the site of action. This relies on measurements of the unbound drug fraction ($f_{u,\text{brain}}$), which currently requires access to brain tissue. Here, we present a novel methodology using homogenates of cultured cells for rapid estimation of $f_{u,\text{brain}}$. In our setup, drug binding to human embryonic kidney cell (HEK293) homogenate was measured in a small-scale dialysis apparatus. To increase throughput, we combined drugs into cassettes for simultaneous measurement of multiple compounds. Our method estimated $f_{u,\text{brain}}$ with an average error of 1.9-fold. We propose that our simple method can be used as an inexpensive, easily available and high-throughput alternative to brain tissues excised from laboratory animals. Thereby, estimates of unbound drug exposure can now be implemented at a much earlier stage of the drug discovery process, when molecular property changes are easier to make.



■ INTRODUCTION

Local drug exposure in the central nervous system (CNS) is a major determinant of drug effects in the brain. Historically, compounds acting on the CNS have been designed to achieve high total concentrations in the brain (high $K_{p,\text{brain}}$ or log BB, the ratio between total brain and plasma drug concentration¹). However, an increase in $K_{p,\text{brain}}$ does not always result in increased efficacy since only the unbound drug can interact with therapeutic targets.^{2,3} Similarly, target affinity in biochemical assays may not translate to efficacy in cell-based or in vivo systems, if increases in affinity are counteracted by a decreased access to unbound drug. Consequently, knowing the unbound drug exposure is instrumental for the optimization of drug efficacy.

Measuring unbound drug concentrations in the brain directly is analytically challenging^{4,5} and not suited for high-throughput formats. Instead, the unbound drug fraction in the brain ($f_{u,\text{brain}}$) is combined with measurements of total concentrations in the brain to approximate unbound drug concentrations in the whole brain ($K_{p,\text{uu,brain}}$)⁶ or in brain cells.⁷ $f_{u,\text{brain}}$ is routinely measured using dialysis of whole-brain homogenate.⁸ Recently, porcine brain membrane vesicles have been proposed as an alternative to dialysis for the estimation of binding.⁹ Although this methodology increases throughput

compared to dialysis, it still requires access to lipid membranes from brain tissue. We recently showed that drug binding in a commonly used cell line, HEK293, was predictive of binding in several liver-derived systems, including microsomes ($r^2 = 0.88$) and rat and human hepatocytes ($r^2 = 0.84$ and 0.91 , respectively).¹⁰ We hypothesized that a similar correlation could exist for binding in brain tissue. If so, the use of HEK293 would increase assay capacity and reduce the number of animals used.

Here, we present a simple, high-throughput method for estimation of $f_{u,\text{brain}}$. The method allows cassette-mode measurement of drug binding in a 96-well format. Our results show that cultured HEK293 cells can be used as a substitute for brain tissue in the determination of $f_{u,\text{brain}}$ during drug discovery.

■ RESULTS

Compound Selection and Data Collection. A set of drug-like compounds ($n = 174$ compounds) for which data on $f_{u,\text{brain}}$ were available was compiled from the literature.^{7,11–13} A

Received: December 20, 2013

Published: March 6, 2014

subset of compounds ($n = 46$) was selected to compare with binding to HEK293 cells.

To ensure that both sets were representative of the chemical space of currently approved drugs, their physicochemical properties were compared with a larger data set ($n = 886$)¹⁴ (Table 1). All three data sets had similar distributions of

Table 1. Physicochemical Characteristics of the Data Sets^a

	small-molecule drug space ^b	collected brain-binding data set	selected representative subset
n	886	174	46
$f_{u,brain}^c$	n.d.	0.22 ± 0.27 (0.00049 – 1)	0.12 ± 0.19 (0.00067 – 1)
MW ^d	372 ± 185 (76 – 1621)	347 ± 143 (129 – 1203)	387 ± 134 (234 – 823)
$\log D_{7.4}^d$	1.1 ± 2.4 (–9.6 – 10)	1.8 ± 1.6 (–2.6 – 5.3)	2.5 ± 1.6 (–0.93 – 4.8)
PSA ^d	91 ± 75 (3.2 – 702)	65 ± 47 (3.2 – 279)	69 ± 47 (6.5 – 217)
major charge species at pH 7.4 ^d			
negative	180 (20%)	13 (7%)	5 (11%)
neutral	333 (38%)	59 (34%)	16 (35%)
positive	269 (30%)	85 (49%)	20 (43%)
zwitterion	104 (12%)	17 (10%)	5 (11%)

^aData are presented as mean \pm SD, with the range in parentheses. ^bFrom Benet et al.¹⁴ ^cCollected from the literature.^{7,11–13} ^dCalculated using ADMET Predictor (Simulations Plus, Lancaster, CA).

compound lipophilicity ($\log D_{7.4}$; Figure 1A), size (molecular weight (MW); Figure 1B), polarity (polar surface area (PSA);

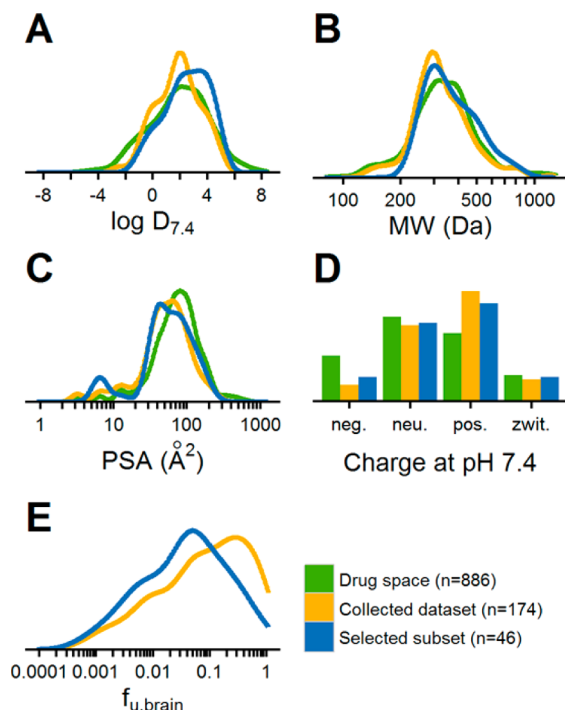


Figure 1. Distributions of calculated physicochemical properties: (A) $\log D_{7.4}$, (B) molecular weight, (C) polar surface area, and (D) most abundant charge species at pH 7.4. (E) Experimental $f_{u,brain}$ of the data sets. Parameter distributions are shown for the full set of brain drug binding data collected from the literature (yellow) and the selected representative subset (blue). The physicochemical properties of a reference set of registered drugs are shown in green.

Figure 1C), and charge (Figure 1D). The mean value of $\log D_{7.4}$ for the selected subset ($n = 46$) was 2.46 ± 1.60 (Table 1), and the mean values of MW and PSA were 387 ± 134 and 68.6 ± 46.6 , respectively. In the 46 compound subset, five were predicted to be negatively charged at pH 7.4, 16 to be neutral, 20 positively charged, and five zwitterionic. The mean \pm SD of $f_{u,brain}$ of the subset ($n = 46$) was 0.12 ± 0.19 (median = 0.043), slightly lower than that of the collected data set ($n = 174$; 0.22 ± 0.27 ; median = 0.091).

Measurement of Drug Binding to Cell Homogenates in Cassette-Mode. Drug binding was measured in homogenates of cultured HEK293 cells, using the method introduced in our recent publication.¹⁰ To increase throughput, drug binding was determined in cassette-mode, i.e., 5–8 compounds were pooled in each experiment. Each cassette was dialyzed in a small-scale setup (48 dialysis membranes per plate), and the compounds were quantified by UPLC–MS/MS. The resulting values of binding to cell homogenates ($f_{u,hom}$) are presented in Table 2.

To ensure that combined compounds would not affect the measurements of cellular binding, they were assigned to cassettes in a randomized manner (Figure S1, Supporting Information). In addition, each compound was measured in three to eight different cassettes (with an average of four measurements per compound). The $f_{u,hom}$ measurements for each compound in different cassettes had a median coefficient of variation of 7.8% (interquartile range (IQR): 5.6–15%; Figure S2, Supporting Information), indicating that the presence of multiple compounds in the cassettes did not particularly affect the results. To further ensure that the cassette-mode did not influence binding measurements, we compared the data with our previously published data¹⁰ where binding was measured for individual compounds (Figure 2). The values were highly correlated ($r^2 = 0.98$, $p < 0.0001$), indicating no difference between cassette and individual measurements.

Comparison between Cellular and Brain Drug Binding. Measurements of $f_{u,hom}$ were transformed into $f_{u,brain}$ predicted with eq 2 so that we could make subsequent comparisons with literature $f_{u,brain}$ data. The scaling factor D in eq 2 was used to account for differences in binding capacity between the two systems, and it was optimized to minimize the systematic bias in predictions that would result from such differences. The optimization was performed independently for 100,000 randomly assigned training sets, each consisting of 30 compounds from the experimental data set. For each permutation, the remaining 16 compounds were used to evaluate the resulting correlation.

This optimization procedure resulted in an average value of $D = 62 \pm 5.9$. Thirty-four of the 46 compounds measured in cell homogenates (74%) were within 2-fold of the values measured in brain and 40 (87%) were within 3-fold (Table 2 and Figure 3). Binding in the brain was moderately underpredicted for zwitterionic compounds at pH 7.4 (AFE = 0.4), while the other charge categories (anionic, cationic, and uncharged compounds) were slightly overpredicted (AFE \approx 1.1). Aside from charge, no other trends in physicochemical characteristics were evident for the deviations (Figure S3, Supporting Information).

DISCUSSION AND CONCLUSIONS

The compounds selected for the brain-binding model were representative of small-molecule drug space in terms of

Table 2. Physicochemical Properties, Binding to Cell Homogenates, and Brain Drug Binding of the Studied Compound Subset^a

compd	MW ^b	log D _{7.4} ^b	PSA ^b	f _{u, hom}	f _{u, brain predicted} ^c	f _{u, brain}	refs
Negatively Charged at pH 7.4							
Chlorpropamide	277	1.38	75.3	1 ± 0.040	1	0.58	d
Diclofenac	296	1.56	49.3	0.78 ± 0.045	0.054	0.041	e
Indomethacin	358	0.74	68.5	0.79 ± 0.035	0.055	0.044	d,e
Sulfasalazine	398	-0.15	138	0.72 ± 0.12	0.039	0.063	e
Telmisartan	515	3.62	72.9	0.42 ± 0.011	0.011	0.013	d
Neutral at pH 7.4							
Alprazolam	309	2.62	43.1	1 ± 0.028	1	0.16	e
Amprenavir	506	1.68	131	0.92 ± 0.046	0.16	0.091	f
Carbamazepine	236	2.56	46.3	0.97 ± 0.11	0.31	0.18	d,f,g
Diazepam	285	2.88	32.7	0.71 ± 0.050	0.037	0.040	e,f,g
Indinavir	614	3.14	118	0.78 ± 0.016	0.055	0.072	f
Ketoconazole	531	3.91	69.1	0.39 ± 0.031	0.010	0.012	f
Loratadine	383	4.56	42.4	0.12 ± 0.0036	0.0022	0.0020	f
Lovastatin	405	4.49	72.8	0.22 ± 0.024	0.0045	0.0080	f
Midazolam	326	3.56	30.2	0.66 ± 0.025	0.030	0.022	e,f,g
Nelfinavir	568	4.71	102	0.024 ± 0.0033	0.00039	0.0021	e,f
Nicardipine	480	4.82	114	0.095 ± 0.013	0.0017	0.0055	d
Ondansetron	293	2.05	39.8	0.94 ± 0.019	0.19	0.049	f
Oxazepam	287	2.18	61.7	0.84 ± 0.024	0.078	0.037	f
Progesterone	314	3.77	34.1	0.67 ± 0.11	0.031	0.046	f
Ritonavir	721	4.56	146	0.47 ± 0.013	0.014	0.018	d,f
Saquinavir	671	4.16	167	0.17 ± 0.011	0.0032	0.0028	e,f
Positively Charged at pH 7.4							
Alprenolol	249	0.61	41.5	0.90 ± 0.031	0.12	0.057	e
Bupivacaine	288	3.67	32.3	0.89 ± 0.068	0.11	0.20	d
Cimetidine	252	-0.37	88.9	1 ± 0.036	1	0.63	e,f
Citalopram	324	1.85	36.3	0.81 ± 0.026	0.064	0.042	d,f,g
Clomipramine	315	3.96	6.48	0.19 ± 0.0083	0.0038	0.0039	d
Dextromethorphan	271	2.51	12.5	0.82 ± 0.019	0.069	0.20	f
Haloperidol	376	2.88	40.5	0.52 ± 0.0092	0.017	0.0065	f,g
Imipramine	280	3.26	6.48	0.59 ± 0.013	0.022	0.035	f
Lidocaine	234	1.87	32.3	0.998 ± 0.0085	0.91	0.27	d
Loperamide	477	4.66	43.8	0.35 ± 0.014	0.0083	0.0094	e,f
Metoclopramide	300	0.53	67.6	0.95 ± 0.068	0.25	0.24	d,f,g
Metoprolol	267	0.05	50.7	1.00 ± 0.056	0.88	0.46	e
Paroxetine	329	1.83	39.7	0.25 ± 0.0085	0.0053	0.0036	d,g
Propranolol	259	1.17	41.5	0.70 ± 0.053	0.036	0.020	e,g
Ranitidine	314	0.15	86.3	1 ± 0.070	1	0.96	f
Spiperone	395	2.17	52.7	0.66 ± 0.014	0.030	0.037	f
Talinolol	364	1.57	82.6	0.85 ± 0.022	0.083	0.14	d
Thioridazine	371	4.3	6.48	0.049 ± 0.0087	0.00082	0.00067	e
Trimipramine	294	3.59	6.48	0.40 ± 0.016	0.010	0.0070	f
Verapamil	455	3.86	64	0.73 ± 0.019	0.041	0.041	e,f
Zwitterionic at pH 7.4							
Cerivastatin	460	2.15	99.9	0.55 ± 0.0094	0.019	0.048	f
Fexofenadine	502	3	81	0.78 ± 0.029	0.054	0.078	f
Mitoxantrone	444	-0.93	163	0.13 ± 0.019	0.0024	0.0046	e
Rifampicin	823	2.93	217	0.62 ± 0.083	0.025	0.13	e
Sparfloxacin	392	-0.76	101	0.88 ± 0.068	0.10	0.26	f

^aExperimental data (f_{u, hom}) are presented as mean ± SD. ^bCalculated using ADMET Predictor (Simulations Plus, Lancaster, CA). ^cPredicted from f_{u, hom} using eq 2. ^dRef 11. ^eRef 7. ^fRef 12. ^gRef 13.

physicochemical properties (Figure 1). The method should thus be applicable to other drug-like compounds within this chemical space. Our previous observations showed that binding to HEK293 cells is mainly driven by nonspecific binding and is not saturable up to 100 μM.¹⁰ Accordingly, we postulated that increasing the number of compounds in each dialysis measurement would not affect the binding at the low drug

concentrations used (0.1 μM). Indeed, the cassette-mode measurements were in excellent agreement with historical values obtained with single compounds¹⁰ (r² = 0.98; Figure 2). By randomly assigning compounds to different cassettes, we also observed a high precision (median coefficient of variation = 7.8%), similar to that observed in our previous measurements of single compounds (8.9%).¹⁰ These levels of variation are

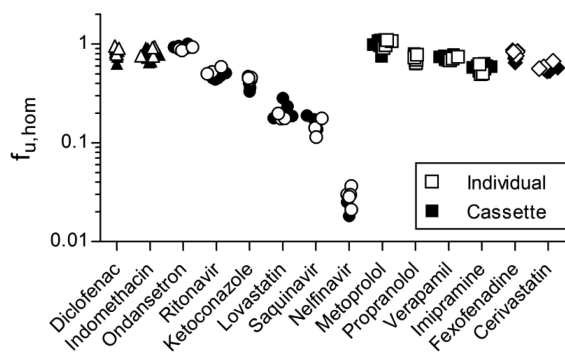


Figure 2. Comparison between drug binding measured in cassette-mode and in incubations with individual compounds ($r^2 = 0.98$). Data for individual measurements are previously published.¹⁰ Negatively charged compounds at pH 7.4 are represented by circles, neutral compounds by triangles, positively charged compounds by squares, and zwitterionic compounds by diamonds. Each point represents a single measurement at one independent occasion.

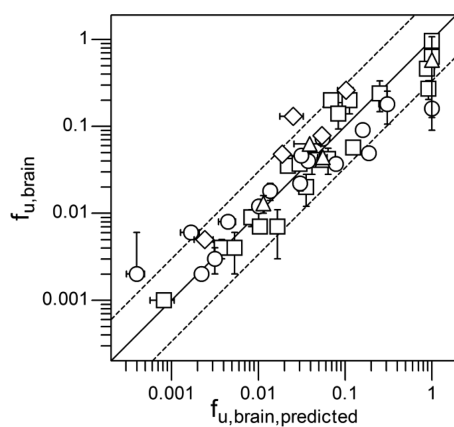


Figure 3. Relationship between $f_{u, \text{brain, predicted}}$ (from HEK293 cell homogenates) and experimental $f_{u, \text{brain}}$ (from brain homogenates) (RMSE = 0.31). Negatively charged compounds at pH 7.4 are represented by triangles, neutral compounds by circles, positively charged compounds by squares, and zwitterionic compounds by diamonds. The solid line represents a perfect prediction, and the dashed lines represent a 3-fold error interval.

lower than those from other laboratories using brain homogenates (median coefficient of variation of the collected data set = 14%).^{7,11,13} Cassette-mode measurement in the miniaturized dialysis assay allows for the measurement of up to 384 compounds per plate (8 compounds \times 48 dialysis membranes). The assay is readily automated, and parallel incubations can increase assay throughput to >1000 compounds/day, limited mainly by analytical capacity.

For comparisons between $f_{u, \text{hom}}$ and $f_{u, \text{brain}}$ unbiased by system-dependent differences in binding capacity (i.e., different concentrations of binding sites), a scaling adjustment was required⁸ (eq 2). The scaling factor ($D = 62$) was therefore specific to the setup in our laboratory. When applying our technique in other laboratories, D should be adjusted accordingly. After proper scaling, our approach predicted $f_{u, \text{brain}}$ within a 2-fold of that measured in brain for 74% and within 3-fold for 87% (RMSE = 0.31) of the compounds.

In our previous study,¹⁰ we showed that drug binding in HEK293 cells correlated well with that in liver-derived tissues. The fact that a commonly used cell line can mimic binding in tissues as different as liver and brain is surprising and led us to

hypothesize that a similar mechanism drives the binding (most likely partitioning to membrane and other lipophilic species, e.g., lipoproteins). In support of this hypothesis, we found that molecular descriptors related to membrane partitioning were inversely correlated to f_u in HEK293 cells.¹⁰ This role of membrane partitioning is also supported by the good correlation between binding to pure membrane vesicles and brain tissue⁹ and by the difficulty involved in saturating this system, e.g., by increasing the concentration of compounds.¹⁰ We speculate that binding to other mammalian tissues can be predicted using a cell line surrogate, provided that the correct scaling factor is used to account for the differences in binding capacity.

In conclusion, we show that our method is rapid, accurate, and precise. The method is also inexpensive and generally applicable in any cell culture laboratory. It therefore has the potential to allow high-throughput screening of $f_{u, \text{brain}}$ at an earlier stage in drug discovery than what is possible using brain homogenates. Further, it may contribute to a reduction in the use of experimental animals.

EXPERIMENTAL SECTION

Materials. All cell culture reagents were purchased from Invitrogen (Carlsbad, CA) or Sigma-Aldrich (St. Louis, MO). All compounds were of analytical grade ($\geq 95\%$ purity) and obtained from AstraZeneca (Mölnådal, Sweden), Sigma-Aldrich (St. Louis, MO), or Toronto Research Chemicals (Toronto, Canada). Compounds were dissolved in dimethyl sulfoxide (DMSO) at a concentration of 10 mM (or lower if not soluble; Table S1, Supporting Information) and stored at -20°C .

Cell Cultivation. Human embryonic kidney cells Flp-In-293 (HEK293) were stably transfected with pOG44 and empty pcDNAS/FRT vectors (Invitrogen, Carlsbad, CA) and maintained as previously described.^{10,15} Briefly, the cells were cultivated at 37°C in Dulbecco's modified Eagle's medium supplemented with 10% fetal bovine serum, 2 mM L-glutamate, and $75\ \mu\text{g}/\text{mL}$ Hygromycin B, in a humidified 5% CO_2 atmosphere. Cells were not used beyond 25 passages after the establishment of stable transfectants.

Preparation of Cell Homogenates. Cell homogenates were prepared from HEK293 cells, as described in Mateus et al.¹⁰ In brief, cells were harvested with 0.05% trypsin, centrifuged at $260 \times g$ for 5 min, and washed with Dulbecco's phosphate-buffered saline. After cell counting with a NucleoCounter NC-100 (Chemometec, Allerød, Denmark), the cells were centrifuged once more at $260 \times g$ for 5 min, and the cell pellet was stored at -20°C . On the day of the experiment, the pellet was thawed on ice and resuspended in Hank's buffered salt solution (HBSS) to 10×10^6 cells/mL. This suspension was homogenized using a VCX-500 ultrasonic processor (Sonics & Materials, Newton, CT) at 20% intensity for 10 s.

Measurement of Binding to Cellular Structures. Binding of compounds to cellular material was measured by dialysis. Cell homogenates were spiked with five to eight compounds (for cassette measurements) to a final concentration of $0.1\ \mu\text{M}$ each (or $0.01\ \mu\text{M}$ for nelfinavir, due to its low water solubility). This resulted in a maximum DMSO concentration of 0.03% in the cell homogenates during measurements. Dialysis was performed with a Rapid Equilibrium Dialysis device (Thermo Fisher Scientific Inc., Rockford, IL), as described elsewhere.¹⁰ At the end of the incubation (4 h), an equal volume of nonspiked homogenate or blank buffer was added to the samples from the buffer or homogenate chambers, respectively. Finally, protein was precipitated with 50 nM warfarin (internal standard) in acetonitrile/water (60:40) and centrifuged for 20 min at $2465 \times g$. Compounds in the supernatant were quantified by UPLC-MS/MS, as described below. Mass balance was evaluated at the end of all experiments and was generally $>90\%$.

The unbound drug fraction in the cell homogenate ($f_{u, \text{hom}}$) was calculated according to

$$f_{u, \text{hom}} = \frac{PA_{\text{buffer}}}{PA_{\text{hom}}} \quad (1)$$

where PA_{buffer} is the peak area of compound in the buffer chamber and PA_{hom} is the peak area of compound in the homogenate chamber, both corrected for the peak area of the internal standard in the respective chamber.

Prediction of Drug Binding in Brain ($f_{u, \text{brain}}$) from Cellular Binding Measurements. Given our hypothesis that the cell homogenate can be used as a surrogate for brain homogenate, an equation typically used to correct for homogenate dilution (D)⁸ was applied to calculate the predicted $f_{u, \text{brain}}$ ($f_{u, \text{brain predicted}}$):

$$f_{u, \text{brain predicted}} = \frac{1}{D\left(\frac{1}{f_{u, \text{hom}}} - 1\right) + 1} \quad (2)$$

In the present work, D was used to compensate for the difference in binding capacities of the two systems. D was optimized to minimize systematic biases in the binding correlations. Our experimental data set ($n = 46$) was randomly divided into 100,000 training and test sets ($n = 30$ and 16, respectively). For each of these permutations, D was optimized to give an average fold error (AFE) of prediction of 1. The optimization included data from the respective training sets only, and the test sets were used to evaluate the resulting correlations. This procedure resulted in an average value of D of 62 ± 5.9 (IQR: 58–66). The AFE and RMSE for the test sets were normally distributed, with average values of 1.0 ± 0.23 (IQR: 0.86–1.2; Figure S4B, Supporting Information) and 0.31 ± 0.05 (IQR: 0.28–0.35; Figure S4A, Supporting Information), respectively.

Collection of Brain-Binding Data. We collated $f_{u, \text{brain}}$ data for 174 drug-like compounds from the literature.^{7,11–13} When there was more than one $f_{u, \text{brain}}$ determination for the same compound, the geometric mean of all measurements was used. Measurements from different species were combined when calculating the means in accordance with previous reports showing no systematic disparity in brain drug binding among different species.¹¹

Analytical Techniques. A Waters Xevo TQ MS with electrospray ionization was used to measure compound concentration. The mass spectrometer was coupled to an Acquity UPLC system (Waters, Milford, MA) equipped with a Waters BEH C18 2.1 \times 50 mm (1.7 μm) column at 60 $^{\circ}\text{C}$ and an autosampler at 10 $^{\circ}\text{C}$. The injection volume was 10 μL . The mobile phase was composed of two solvents: solvent A, 5% acetonitrile and 0.1% formic acid in water; and solvent B, 0.1% formic acid in acetonitrile. The chromatographic run consisted of a linear gradient at a flow rate of 0.5 mL/min. The gradient comprised an increase from 5% to 90% of solvent B from 0.5 to 1.2 min, followed by a hold from 1.2 to 1.6 min and a return to the initial conditions at 1.7 min until the end of the run (2 min). Mass transitions and their respective cone voltages and collision energies are in Table S1, Supporting Information.

Molecular Descriptor Generation. Corina version 3.46 (Molecular Networks, Erlangen, Germany) was used to generate three-dimensional molecular structures from SMILES representations (Table S2, Supporting Information). For each compound, up to 100 ring conformations were generated. The conformation with the lowest steric energy (assessed using the internal Corina force field) was used as input for calculation of physicochemical properties using ADMET Predictor, version 6.5 (SimulationsPlus, Lancaster, CA).

Statistics. Experiments were performed on at least three independent occasions. Results are presented as mean \pm standard deviation (SD), unless otherwise stated. Average fold error (AFE) and root-mean-square error (RMSE) were used to assess the quality of the relationship between $f_{u, \text{brain predicted}}$ and $f_{u, \text{brain}}$.

■ ASSOCIATED CONTENT

Supporting Information

Table S1. Analytical conditions for compound quantification; Table S2. Physicochemical characteristics and collected $f_{u, \text{brain}}$ data for 174 compounds; Figure S1. Assignment of compounds

to the test cassettes; Figure S2. Distribution of the coefficient of variation among $f_{u, \text{hom}}$ determinations; Figure S3. Analysis of the distribution of prediction errors for $f_{u, \text{brain}}$. Figure S4. Sensitivity analysis for the scaling factor D . This material is available free of charge via the Internet at <http://pubs.acs.org>.

■ AUTHOR INFORMATION

Corresponding Author

*(P.A.) E-mail: per.artursson@farmaci.uu.se. Tel: +46 18 471 44 71. Fax: +46 18 471 42 23.

Author Contributions

The manuscript was written through contributions of all authors. All authors have given approval to the final version of the manuscript.

Notes

The authors declare no competing financial interest.

■ ACKNOWLEDGMENTS

The authors gratefully acknowledge SimulationsPlus for access to the ADMET Predictor software. The authors also acknowledge the support from Science for Life Laboratory (SciLifeLab). This work was supported by the Swedish Fund for Research Without Animal Experiments, Magnus Bergvalls Stiftelse, and the Swedish Research Council (grant nos. 9478 and 21386). A.M. was supported by a Ph.D. training grant from Fundação para a Ciência e Tecnologia, Portugal (grant no. SFRH/BD/68304/2010).

■ ABBREVIATIONS USED

$f_{u, \text{brain}}$, unbound drug fraction in brain; $f_{u, \text{hom}}$, unbound drug fraction in cellular homogenates; HEK293, human embryonic kidney cells; Kp_{brain} or log BB, ratio between total brain and plasma drug concentration; $Kp_{\text{uu, brain}}$, ratio between unbound brain and plasma drug concentration; HBSS, Hank's buffered salt solution; SMILES, simplified molecular-input line-entry system; AFE, average fold error; RMSE, root-mean-square error

■ REFERENCES

- (1) Boje, K. M. K. In vivo measurement of blood–brain barrier permeability. In *Current Protocols in Neuroscience*; John Wiley & Sons, Inc.: New York, 2001.
- (2) Read, K. D.; Braggio, S. Assessing brain free fraction in early drug discovery. *Expert Opin. Drug Metab. Toxicol.* **2010**, *6*, 337–344.
- (3) Smith, D. A.; Di, L.; Kerns, E. H. The effect of plasma protein binding on in vivo efficacy: misconceptions in drug discovery. *Nat. Rev. Drug Discovery* **2010**, *9*, 929–939.
- (4) Boschi, G.; Scherrmann, J. Microdialysis in mice for drug delivery research. *Adv. Drug Delivery Rev.* **2000**, *45*, 271–281.
- (5) Liu, X.; Smith, B. J.; Chen, C.; Callegari, E.; Becker, S. L.; Chen, X.; Cianfrogna, J.; Doran, A. C.; Doran, S. D.; Gibbs, J. P.; Hosea, N.; Liu, J.; Nelson, F. R.; Szewc, M. A.; Van Deusen, J. Evaluation of cerebrospinal fluid concentration and plasma free concentration as a surrogate measurement for brain free concentration. *Drug Metab. Dispos.* **2006**, *34*, 1443–1447.
- (6) Gupta, A.; Chatelain, P.; Massingham, R.; Jonsson, E. N.; Hammarlund-Udenaes, M. Brain distribution of cetirizine enantiomers: comparison of three different tissue-to-plasma partition coefficients: $K(p)$, $K(p,u)$, and $K(p,uu)$. *Drug Metab. Dispos.* **2006**, *34*, 318–323.
- (7) Fridén, M.; Bergström, F.; Wan, H.; Rehgren, M.; Ahlin, G.; Hammarlund-Udenaes, M.; Bredberg, U. Measurement of unbound drug exposure in brain: modeling of pH partitioning explains diverging results between the brain slice and brain homogenate methods. *Drug Metab. Dispos.* **2011**, *39*, 353–362.

(8) Kalvass, J. C.; Maurer, T. S. Influence of nonspecific brain and plasma binding on CNS exposure: implications for rational drug discovery. *Biopharm. Drug Dispos.* **2002**, *23*, 327–338.

(9) Longhi, R.; Corbioli, S.; Fontana, S.; Vinco, F.; Braggio, S.; Helmdach, L.; Schiller, J.; Boriss, H. Brain tissue binding of drugs: evaluation and validation of solid supported porcine brain membrane vesicles (TRANSIL) as a novel high-throughput method. *Drug Metab. Dispos.* **2011**, *39*, 312–321.

(10) Mateus, A.; Matsson, P.; Artursson, P. Rapid measurement of intracellular unbound drug concentrations. *Mol. Pharmaceutics* **2013**, *10*, 2467–2478.

(11) Di, L.; Umland, J. P.; Chang, G.; Huang, Y.; Lin, Z.; Scott, D. O.; Troutman, M. D.; Liston, T. E. Species independence in brain tissue binding using brain homogenates. *Drug Metab. Dispos.* **2011**, *39*, 1270–1277.

(12) Lanevskij, K.; Dapkunas, J.; Juska, L.; Japertas, P.; Didziapetris, R. QSAR analysis of blood-brain distribution: the influence of plasma and brain tissue binding. *J. Pharm. Sci.* **2011**, *100*, 2147–2160.

(13) Wan, H.; Rehngren, M.; Giordanetto, F.; Bergström, F.; Tunek, A. High-throughput screening of drug-brain tissue binding and in silico prediction for assessment of central nervous system drug delivery. *J. Med. Chem.* **2007**, *50*, 4606–4615.

(14) Benet, L. Z.; Broccatelli, F.; Oprea, T. I. BDDCS applied to over 900 drugs. *AAPS J.* **2011**, *13*, 519–547.

(15) Karlgren, M.; Ahlin, G.; Bergström, C. A.; Svensson, R.; Palm, J.; Artursson, P. In vitro and in silico strategies to identify OATP1B1 inhibitors and predict clinical drug–drug interactions. *Pharm. Res.* **2011**, *29*, 411–426.